



Contribution of seismic tomography for taking soil variability into account in landslide stability numerical modelling

J. Gance (1), S. Bernardie (1), R. Vandromme (1) & G. Grandjean (1)

(1) BRGM – Natural Hazard and CO2 Security Storage Department. E-mail: g.grandjean@brgm.fr, Tel. +33-(0)238643524

ABSTRACT: The Ballandaz landslide (Le Planay, France) has been studied for years. Geotechnical characterization, geophysical surveys and geomechanical modelling have been performed to characterize its behaviour, but these different approaches were not deeply analysed in a common way. This work aims to study what kind of contributions geophysical data could provide in geomechanical modelling. In particular, seismic and borehole data, obtained during previous campaigns, are used for taking into account the soil variability in a finite element modelling. Instead of constructing the slope model from geological interpretations, themselves derived from geophysical sections – as it is generally done – we use the P-wave velocity distribution obtained from seismic tomography computations to fill the mechanical mesh with different mechanical properties. Simulations are carried out with the GEFDYN code. A parametric study is also performed for determining the optimal number of materials, the optimal element size, the velocity classification algorithm, etc. Finally, our results are compared to a classical 3-layers model for discussion.

1 INTRODUCTION

Nowadays, geomechanical finite-element codes running on modern computers allow complex calculations and produce coherent results, particularly when homogeneous media are considered. Taking into account the spatial heterogeneity of geological materials is becoming a new challenge in numerical modeling, since simulating natural processes conform as much as possible to the reality is not straightforward. Some scientific publications deal with such issue, but they are generally focused on stochastic analyses of the problem. These methods give relatively good results for standard slope stability simulations (Cho, 2007; Griffiths & Fenton, 2004; Vanmarcke 1980; Meo et al., 2008) but remain relatively complex to implement and strongly time consuming (Rohmer 2009). Montgomery (1994) showed that the simple introduction of topography in a model allows increasing the potentiality for shallow landslides occurrence.

We propose here a method that takes into account the spatial variability of the different constitutive materials of a slope - and the changes of their mechanical properties - from seismic tomographic images. To measure the pertinence of such approach,

we compare it with a simple 3-layers model that is generally used for standard numerical studies.

The work is divided into two parts. The first one presents how the 2D numerical mesh modeling the slope is automatically generated from the P-wave velocity (V_p) tomogram (Grandjean & Sage, 2004). For this aspect, the numerical mesh is composed of a given number of materials, each material being characterized by several mechanical parameters. These parameters are estimated from petrophysic relationships depending on the V_p quantity.

The second part presents a parametric study where different algorithm options entering in the computations are tested with the GEFDYN code (Aubry et al., 1986). The main goal of this study being dedicated to measure the reliability of our approach in the context of heterogeneous slopes, we finally compare the final cross-section of the failure criterion to field observations.

2 AUTOMATIC CREATION OF THE MODEL

2.1 Creation of the mesh

A transformation routine is used for creating the mechanical mesh. It uses directly the V_p seismic tomogram to build a numerical mesh taking into account the topography, each element being

characterized by a V_p value. Then, a k-means classification (Ding and He, 2004) algorithm is used to confer a material number to each elements, the total number of material being arbitrary fixed.

Each material is attributed to a group by the same algorithm so that the materials belonging to a group have some mechanical properties in common (Figure 1). The number of group is also arbitrary fixed.

2.2 Determination of the hydro-mechanical parameters

After the mesh has been created, the program attributes to each material the values of 9 hydro-mechanical parameters necessary to define the Drucker-Prager constitutive law in GEFDYN:

- P-wave velocity (V_p)
- Poisson coefficient (ν)
- Young modulus (E)
- Density (ρ)
- Porosity (n)
- Permeability (k)
- Cohesion (c)
- Friction coefficient (f)
- Earth pressure coefficient (K_0)

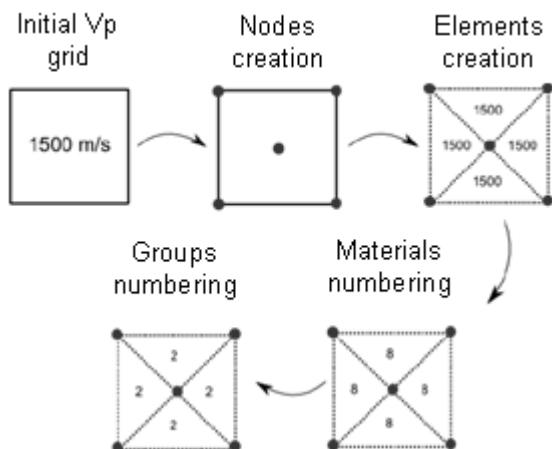


Figure 1. Creation of a mesh from the V_p data grid.

Four of these parameters are identical to all materials composing a group: the solid density, the cohesion, the friction angle and the Poisson ratio. If the model is constituted of 3 groups, three different sets of parameters need to be specified. The other parameters are supposed to vary spatially within a specific material; they are estimated for each of them from the V_p values and the constant parameters of the group. Different petrophysical relationships were used for this estimation, knowing that they are valid for most of rocks.

The parameters derived from V_p are the following:

- The porosity ϕ : it is calculated with the relation proposed by Castagna (1985):

$$V_p = 5810 - 9420 \cdot \phi - 2210 \cdot V_{cl} \quad (1)$$

where ϕ refers to the porosity in percent, V_{cl} , the clay volume in percent. V_{cl} is taken equal to zero to keep a good range of porosity in the model.

- The Young modulus E : it is calculated with a relation restricted to isotropic homogeneous medium:

$$E = V_p^2 \cdot \rho \cdot \frac{(+\nu)(-2 \cdot \nu)}{(-\nu)} \quad (2)$$

- The permeability k is calculated with the relation proposed by Berg (1970):

$$k = 5,1 \cdot 10^{-6} \cdot \phi^{5,1} \cdot d^2 \cdot \exp(-1,385 \cdot \phi) \quad (3)$$

Where k is the permeability in darcy; ϕ is porosity in percent, d is median diameter of grains in mm, ϕ is the standard deviation and equals to $P_{90} - P_{10}$.

We choose, after calibration, $\phi = 0$ and $d = 0.12$ mm. The coefficient of earth pressure at rest is calculated from the friction angle f :

$$K_0 = 1 - \sin f \quad (4)$$

The friction angle will be taken under 35.3° for the good accuracy of the results (Desrues 2002).

Figure 2 (top) shows the mesh constituted by the three different groups, each group containing a certain number of materials (non-visible here).

Figure 2 (bottom) shows the classical 3-layers model that will be used to compare.

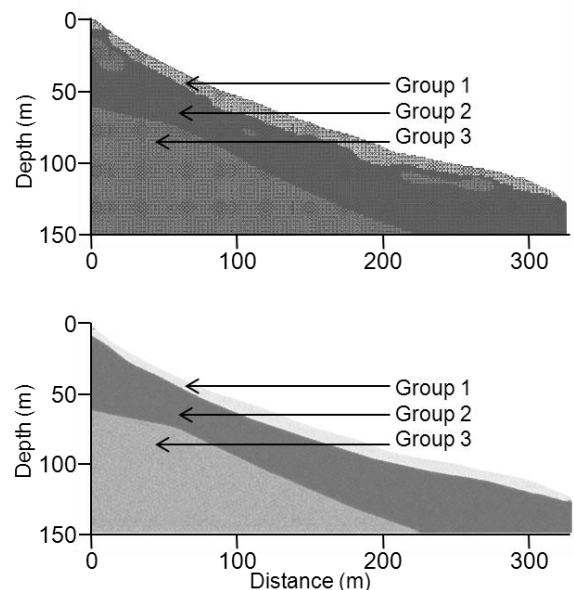


Figure 2. Model created automatically from the V_p data grid (top). 3-layers model used for the comparison.

2.3 Boundary conditions

The calculations were carried out with the Drucker-Prager constitutive law defined in the GEFDYN finite-elements code, using the plane strain approximation. Vertical displacements and horizontal ones were respectively fixed at the lower edge of the mesh and at the left one. The right edge was assumed to be free of displacements for the strength not to be constrained (Figure 3a).

In the case of hydro-mechanical calculation, the pore pressure is imposed at each node. We model the presence of water using a linear water table. All the pressures imposed are hydrostatic ones (Figure 3b). The simulation then refers to a non-coupled hydro-mechanical calculation.

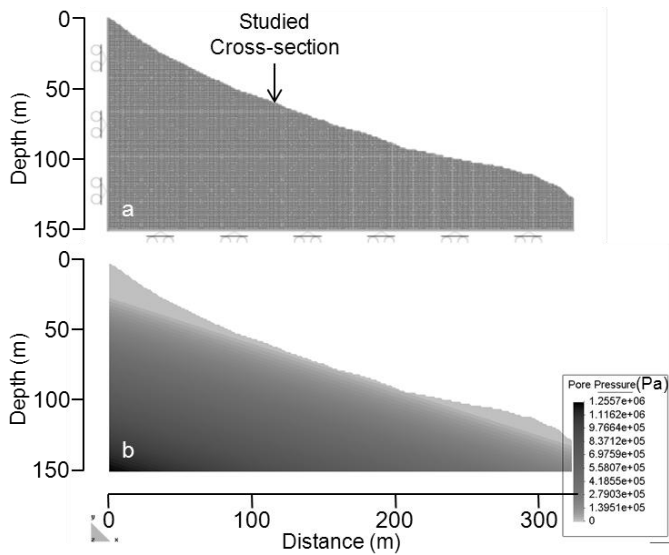


Figure 3. a) conditions on displacements, and b) imposed pore pressure.

3 RESULTS OF CALCULATIONS

3.1 Preliminary tests on the size of the elements and the number of materials

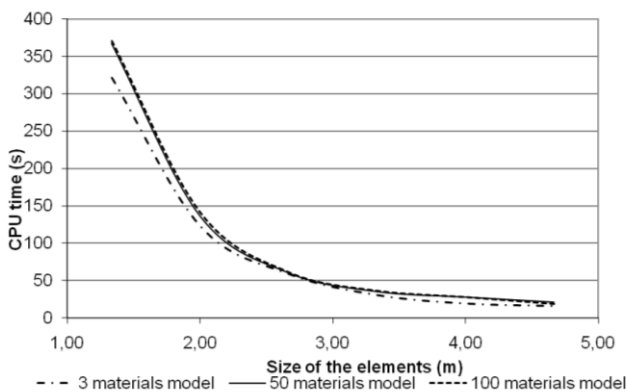


Figure 4. CPU time in function of the size of the elements for different numbers of materials.

A first simple study shows that the number of materials doesn't change very much computing times, contrary to the size of the elements, as clearly shown in Figure 4. On the other hand, the size of elements plays a role in the quality of the results. This value was adjusted to 1.3 m, for avoiding the numerical artifacts due to the mesh roughness without increasing the computation times too much.

3.2 Failure criterion

In order to visualize the potential failure of the slope, we need to define a failure criterion. The most commonly used is the Mohr-Coulomb one, but it can be out of range in the case of low normal stresses. The introduction of the parabolic criterion of Lade (2010) can correct this problem:

$$\tau = a \cdot Pa \cdot \left(\frac{\sigma'}{Pa} \right)^b \quad (5)$$

With τ is the tangential stress, σ' the effective normal stress, Pa the atmospheric pressure, a and b two dimensionless coefficients.

This Θ criterion is simply based on the assumption that it fits the Mohr-Coulomb criterion for maximum stresses (Figure 5) but drops to zero for null stresses. The a et b coefficients are chosen so that the two curves are superimposed for normal stresses higher than 50 kPa. The failure is studied only on horizontal facets. For avoiding to mix two criteria (parabolic and Drucker-Prager criteria), the computations are realized in the elastic domain. The following equation represents the distance to the criterion:

$$\begin{cases} \tau - \tau_{crit} & \text{if } \tau > \tau_{crit} \\ 0 & \text{if } \tau < \tau_{crit} \end{cases} \quad (6)$$

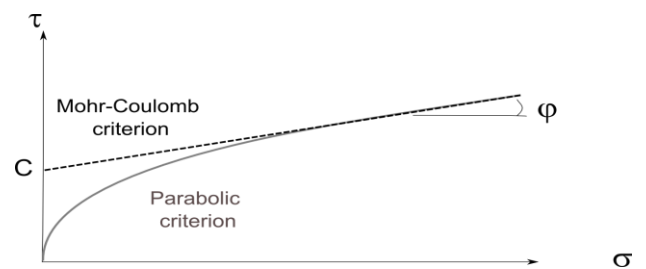


Figure 5. The parabolic θ and Mohr-Coulomb criteria represented in the Mohr plane.

3.3 Comparing the 3-layers model and the automatic one.

We compare here the impact of the two following models on the simulation results:

- The model 1: a 3-layers model, created by hand, and contains 3 materials;
- The model 2: generated automatically from V_p values, and contains 3 materials too.

For this last case, properties of each material are calculated from Vp values according to equations 1 to 4 (Table 1).

Table 1. Parameter fixed for each group.

| Property | Material 1 | Material 2 | Material 3 |
|----------------|------------|------------|---------------------------|
| Poisson ratio | 0.3 | 0.2 | 0.17 |
| Solid density | 1800 | 2200 | 2400 (Kg/m ³) |
| Friction angle | 35° | 29° | 29° |
| Cohesion | 10 | 300 | high (kPa) |

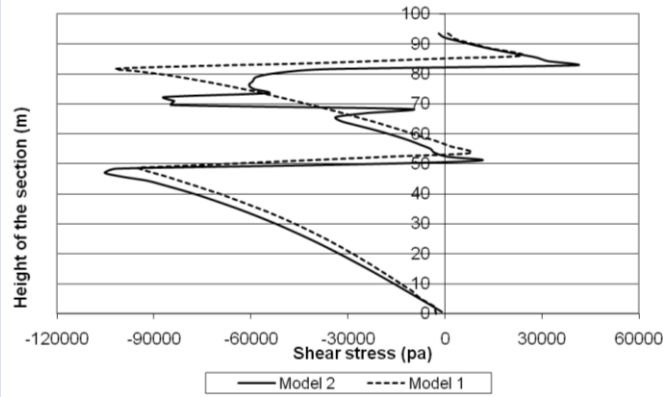


Figure 6. Shear stress on the cross section X=110m.

Let's analyze stress variations along a vertical section for the two models (Figure 6). We can notice that results are quite similar in the homogeneous zones for both of them, but some differences are visible at the interfaces. Indeed, the model 2 presents some high shear stress picks at the interface of heterogeneities that are not present in the model 1. Moreover, the higher stress values observed at the interfaces of materials are deeper for the model 2 than for the model 1.

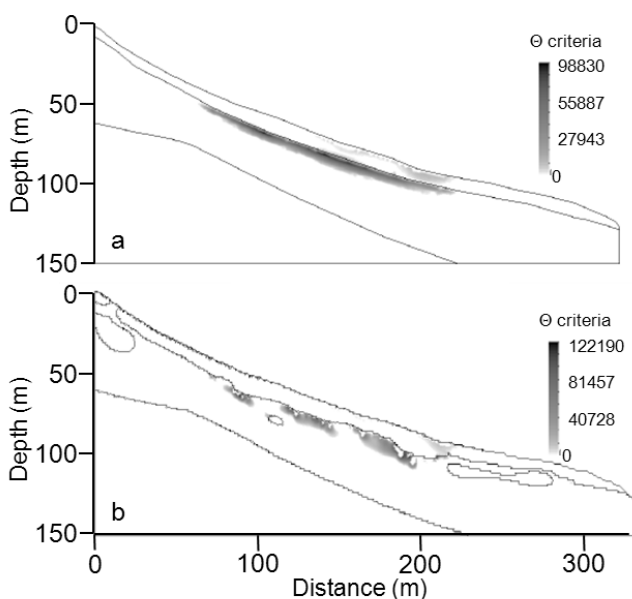


Figure 7. Localized failures in the case of model 1 (a) and model 2 (b)

As a first conclusion, we can highlight that the simple consideration of the materials spatial variability - that represents the only difference between the two models - can strongly modify the slope behavior. Instead of giving a large zone of failure, the calculation with model 2 shows three localized zones situated in the second material at the places where some heterogeneities are observed (Figure 7).

4 PARAMETRIC STUDY

4.1 The number of materials

In this part, we study the impact of the number of materials used in the model. By setting a large number of materials, we expect to take into account the smooth variations of hydro-mechanical properties, as shown on the Vp tomogram, avoiding consequently sharp variations between two consecutive materials.

Six different automatically generated models have been tested with a number of materials comprised between 3 and 100. The results show that the places of the potential failure are affected by this number. We can see for example that the failure zones are deeper (1 to 5 meters) with a large number of materials as shown on Figure 8. We will see later that this representation of the failure plane fits quite well with the field data. The amplitude of the strength is also higher in the 3-layers model than in the others. This could be due to strength artifacts located near the interfaces separating too contrasted materials as it is the case for the 3-layers model. Moreover, the comparison between the Figure 7 and Figure 8 shows that a high number of material smoothes the result and then give more coherent stresses. Indeed, in the classical 3-layers model, the failure appears as guided by the layered structure, leading to artifacts in some places, whereas in the 100 materials model the failure zones are larger and more regular.

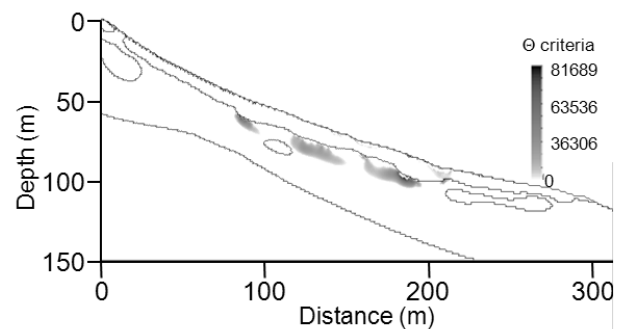


Figure 8. Failure criterion on a 100 material model.

Evidently, a high number of materials seems more appropriate to model this kind of slope. For the rest of the studies, we will use 100 materials.

4.2 Variation of the cohesion inside a group.

The cohesion cannot be estimated from V_p values. To ensure a strong continuity of strength within the model, we tried to smooth the cohesion linearly between materials of two neighboring groups. The two extreme values were taken so that the Drucker-Prager criterion is reached in the first group and the failure is located in the second one. As shown on Figure 9, the strengths are now smoothed at the interfaces and the contrast of stresses between two materials is lower. In addition, the convergence of computations was better.

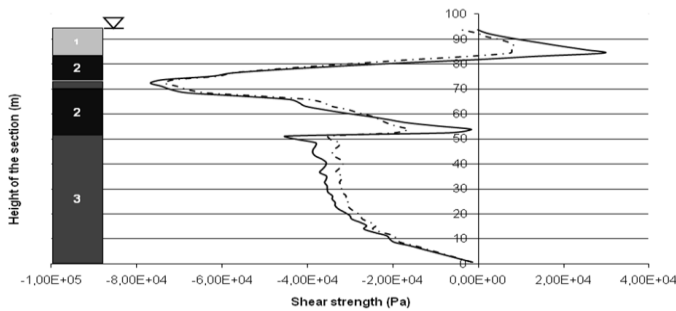


Figure 9. Shear strength on the cross section X=110m for fixed cohesion (solid line) and linear variation of cohesion (dot line)

4.3 Test on the classification algorithms

In order to understand the impact of the classification of materials, we have also tested 3 different algorithms. The k-means algorithm was compared to two other ones that (i) separates the V_p in classes of the same size and (ii) creates classes that contain the same number of elements. These algorithms have been chosen to be very different in order to highlight their impact on the results. After the tests, we can note that this impact is quite negligible. The shear strength is slightly different only in the downhill part of the slope of about 6%. This difference seems not to be due to the change of the geometry since we use a 100 materials model. It is more related to the change of the V_p values attributed to each material, and then to the change of the mechanical parameters.

Finally, the effects of the classification algorithm on the simulation are minor in the case of a 100 materials model. This test also shows that a variation of mechanical properties in the materials has not always a notable effect on the resulting strength. We will thus keep the k-means algorithm for the rest of the study.

4.4 Conclusions on the automatically created model

We saw that the automatic constructed model allows the integration of V_p variations observed in the tomogram, and thus takes into account the spatial variability of the medium heterogeneities after they have been translated into mechanical properties.

The principal drawback of the method concerns the artifacts due to crenellated boundaries separating the materials: these artifacts impact the simulations, particularly when the size of the elements is large and when the number of material is low. In order to minimize those artifacts, we built a model with a shorter size of elements and with a higher number of materials. These new conditions made the resulting images smoother, with a good integration of the spatial variability of properties and a good convergence of the computations.

5 COMPARISON WITH THE FIELD DATA

Two boreholes have been drilled close to the studied profile. The first one (SC1) give a surface of failure at 22 meters of depth. The second one (I4) is not located exactly on the profile, but we expected a surface of failure between 10 and 15 meters of depth just under the road.

We performed a calculation on a 100 materials model, created with all the properties described in the previous paragraph. Then, we calculated the parabolic failure criterion, and from this result, we identified a likely surface of failure on the model (Figure 10). This result was compared to the one obtained from the 3-layers model.

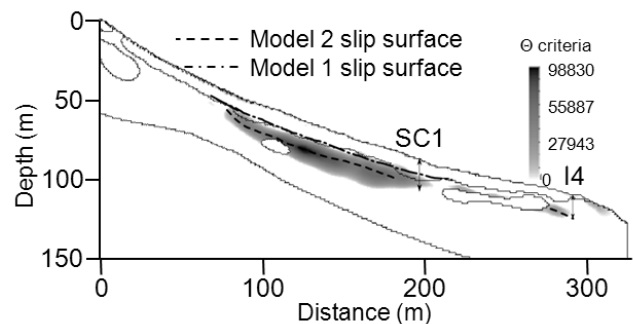


Figure 10. Comparison between two likely surfaces of failures.

We can see that the two identified surfaces are quite different. The surface found using the V_p -oriented model fits better with the field data than the other one. Moreover, the simple 3-layers model doesn't give information under I4, whereas the other one permits to draw a surface around 13m.

6 HETEROGENEITIES IN THE MODEL

To identify the surface of failure as we did in the previous paragraph, we used the parabolic failure criterion, post processed from the strength calculated by the finite elements code GEFDYN. We stated that the V_p -oriented model take into account the heterogeneities, since it is able to consider inclusions

of a strong material in a softer one. The parameters of this heterogeneity are then stronger than those of the soils all around. Nevertheless, the finite elements code handles the inclusions and the bulk material as one. The solution in displacements has to be continuous, and then, doesn't admit the slide of a material on another. That case can be, however, probable in reality.

This problem can be solved in GEFDYN by using a mechanical interface element that allows the slide of a volume on another one, but the difficulty is to automate this process, and in particular to detect such a situation all over the model: not all heterogeneities are supposed to slide on the bulk material situated below.

To finalize our interpretation, we can draw a new surface of failure considering that the slide of the heterogeneity is possible, and make it go just under the downhill block (Figure 11).

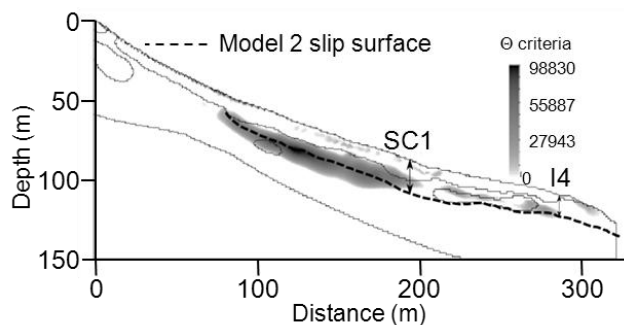


Figure 11. Surface of failure drawn from the result of a calculation on our model. The depths of the surface is written at SC1 and I4

As shown on Figure 11, the depths of the sliding plane in SC1 and I4 areas is well correlated to the simulated maximum of failure.

7 CONCLUSIONS

We tested and developed a method for building a finite-elements model from P-wave velocity values derived from seismic tomography. This approach preserve in the modeling the sliding domains of the slope compared to the common used method that orient them along contrasts of mechanical properties. We have demonstrated that the simple contribution of the geometry of the soil provide rather accurate results.

The first drawback of this method is that the crenellated interface between materials creating artifacts on strength can be limited if a high number of materials is used, and if the contrast of properties between two consecutive materials is low. The study also highlights the difficulty to model properly a medium constituted of several materials with quite different properties. The proposed method solves

this issue by smoothing linearly properties belonging to two contiguous materials. This approach allows a good convergence for high contrasted models, with good accuracy of resulting strength.

Some improvements on the method are still possible. Indeed, we have seen that the role of heterogeneities in the failure were not fully taken into account, and that it was not recommended to model two very contrasted materials, because of the smoothing technique proposed to stabilize the convergence. These aspects should be addressed in the future steps of our work.

Finally it would have been interesting to test some dynamic conditions. For example, the sudden raising of the water table level could modify locally the stresses in the model because of the spatial variability of the permeability.

8 BIBLIOGRAPHIE

- Aubry, D., D. Chouvet, A. Modaressi, and H. Modaressi. 1986. *GEFDYN - Notice Scientifique*. Ecole Centrale PARIS.
- Berg, R. 1970. Method for determining permeability from reservoir rock properties. *Gulf Coast Association in Geological Society Transactions*. 1970, 20, 303-317.
- Castagna, J.P., Batzle, M.L. et Eastwood, R.L. 1985. Relationships between compressional-wave and shear-wave velocities in clastic silicate rocks. *Geophysics*. 50, 4, 571-581.
- Cho, S. E. 2007. Effects of spatial variability of soil properties on slope stability. *Engineering Geology*. 92, 3-4, 97-109
- Desrues, Jacques. 2002. Limitations du choix de l'angle de frottement pour le critère de plasticité de Drucker-Prager. *Revue Française de Géotechnique*, 853-862.
- Ding, C. and He, X. 2004. K-means Clustering via Principal Component Analysis. Proc. of Int'l Conf. Machine Learning (ICML 2004), 225-232.
- Grandjean, G., and S. Sage. 2004. JaTS: a fully portable seismic tomography software based on Fresnel wavepaths and a probabilistic reconstruction approach. *Computers and Geosciences* 30, 925-935.
- Griffiths, D.V., and Gordon A. Fenton. 2004. Probabilistic slope stability analysis by finite elements. *Journal of the Geotechnical Engineering Division, ASCE* 130, 5, 507-518.
- Meo, M., U. Tamaro, and P. Capuano. 2008. Influence of topography on ground deformation at Mt. Vesuvius (Italy) by finite element modelling. *Non-linear Mechanics*. 43, 3, 178-186.
- Montgomery, David R. 1994. A physically based model for the topographic control on shallow landsliding." *Water Resources Research*, 30, 4, 1153-1171.

Rohmer, Jeremy. 2009. Développement d'une méthodologie de propagation de champ aléatoires dans les modèles éléments finis. *Journées Vulnerisc* Orléans, France, 2009.

Lade, V. P. 2010. The mechanics of surficial failure in soil slopes. *Engineering Geology*, 114, 1-2, 57-64.

Vanmarcke, E.H. 1980. Probabilistic stability analysis of earth slopes. *Engineering Geology*. 16, 1-2, 29-50.